electronics

MDPI

Article

Evaluation of Velocity Signals Measured by Laser in Hydrophone Calibration Based on a Normalized Dynamic Time-Warping Algorithm

Xiaowei Liu [1,2], Haijiang Zhu [1], Min Wang [2,*], Ping Yang [2,*], Ke Wang [2] and Longbiao He [2]

[1] College of Information Science and Technology, Beijing University of Chemical Technology, Beijing 100029, China; 2022400210@buct.edu.cn (X.L.); zhuhj@mail.buct.edu.cn (H.Z.)
[2] Division of Mechanics and Acoustics Metrology, National Institute of Metrology, Beijing 100029, China; wangke@nim.ac.cn (K.W.); helb@nim.ac.cn (L.H.)
* Correspondence: wangmin@nim.ac.cn (M.W.); yangp@nim.ac.cn (P.Y.)

Abstract: Laser heterodyne interferometry plays a crucial role in measuring the velocity of water particles during the calibration of hydrophones with the optical method. The velocity of water particles acts as an indicator of acoustic-pressure variations and can be used to evaluate the stability of the acoustic field. The calibration of hydrophones requires a stable acoustic field environment; currently, though, the assessment of acoustic field stability is largely subjective. This study introduces the Normalized Dynamic Time-Warping (NDTW) algorithm, which objectively evaluates acoustic field stability. Sine-fitting is applied to the region of interest in the measured signal to obtain a reference signal. Subsequently, the NDTW algorithm is used to calculate the difference between the measured and reference signals, enabling the assessment of acoustic field stability. The NDTW algorithm effectively identifies subtle differences between signals and addresses the accumulation errors arising from varying signal lengths. The calibration results showed that for signals of high quality within the identified frequency band, the calibration outcomes obtained using the NDTW algorithm deviated from the reciprocity method by no more than 0.7 dB. For frequency bands with poor signal quality identified by the NDTW algorithm, the deviation between the calibration results and the reciprocity method exceeded 0.7 dB.

Keywords: normalized dynamic time warping; signal assessment; evaluation of velocity signals

check for updates

Academic Editor: Yide Wang

Received: 22 November 2024
Revised: 10 January 2025
Accepted: 16 January 2025
Published: 18 January 2025
Corrected: 27 March 2025

Citation: Liu, X.; Zhu, H.; Wang, M.; Yang, P.; Wang, K.; He, L. Evaluation of Velocity Signals Measured by Laser in Hydrophone Calibration Based on a Normalized Dynamic Time-Warping Algorithm. *Electronics* **2025**, *14*, 369. https://doi.org/10.3390/electronics14020369

Copyright: © 2025 by the authors. Licensee MDPI, Basel, Switzerland. This article is an open access article distributed under the terms and conditions of the Creative Commons Attribution (CC BY) license (https://creativecommons.org/licenses/by/4.0/).

1. Introduction

Laser Doppler velocity measurement is a non-invasive technique that is unaffected by the size, temperature, or positional constraints of the object under measurement [1]. It offers numerous advantages, such as extended measurement distance, high spatial resolution, brief measurement duration, and the absence of additional mass in the object. Therefore, it is extensively utilized in mechanical diagnostics [2], structural monitoring [3], and the modal analysis of aerospace structures [4], as well as in acoustic characterization [5] and measurement.

The calibration of hydrophones by optical methods constitutes a pivotal research area for next-generation hydrophone calibration, encompassing optical techniques for measuring underwater acoustic pressure [6]. A transparent pellicle is placed at the measurement site, with a reflective coating applied to one of its surfaces [7]. By employing the Laser Doppler Vibrometer (LDV) to evaluate the pellicle's velocity, variations in underwater

acoustic pressure are reflected in the pellicle's response [8]. By measuring both the underwater acoustic pressure and the hydrophone voltage at the designated location, the sensitivity of the hydrophone can be determined, thus achieving the calibration of the hydrophone [9].

The calibration of hydrophones necessitates a stable free-field environment, as the stability of the acoustic field directly influences the accuracy of the measurement results. In the reciprocity method of calibration, underwater acoustic pressure is inferred indirectly rather than measured directly. Due to the limitations imposed by the response bandwidth and size of the hydrophone, it becomes challenging to directly evaluate the stability of the acoustic field solely based on the signal received by the hydrophone. In the calibration with the optical method, the pellicle can effectively track the velocity of water molecules, and these velocities are measured using a Laser Doppler Vibrometer to calculate the acoustic pressure. Consequently, the stability of the acoustic field can be assessed directly through the analysis of the velocity signal emanating from the pellicle. This method allows for a quantitative evaluation of the acoustic field's stability, as the velocity signal of the pellicle provides a direct indication of any perturbations or variations in the acoustic field.

Presently, signal quality assessment predominantly relies on reference signals, and the precise evaluation of measurement signal quality is attained through the comparison of characteristic disparities between the measurement and reference signals. The primary evaluation methods for one-dimensional signals include the Cross Correlation (Xcorr), Pearson Correlation Coefficient, Jaccard–Tanimoto Coefficient, and Euclidean Distance (ED) methods. Cross Correlation is a technique for assessing the similarity between two signals by computing the correlation at various time delays, thereby identifying the delay that maximizes their similarity [10]. The Pearson Correlation Coefficient is primarily utilized to assess the magnitude and direction of the linear relationship between two variables, enabling the effective inference of data correlation [11]. The Jaccard–Tanimoto Coefficient, grounded in set theory principles, determines the similarity between two sets by computing the ratio of their intersection to their union [12]. Within the realm of data mining, the Jaccard–Tanimoto Coefficient is extensively employed as a similarity measurement method in tasks including clustering and classification. Euclidean Distance (ED) is a metric that quantifies the degree of similarity or dissimilarity between two signals and is utilized to measure the extent of difference between them in a multidimensional space. It finds widespread application in domains including pattern recognition, data mining, and signal processing.

The assessment methodologies for two-dimensional signals include the Peak Signal-to-Noise Ratio (PSNR), Mean Squared Error (MSE), Mahalanobis Distance, and Dynamic Time-Warping (DTW) methods. PSNR serves as a metric prevalently used in evaluating the fidelity of reconstructed signals through comparison with the original. It is frequently employed for the swift evaluation of image and video quality and has been extensively integrated into numerous image and video coding standards. MSE quantifies the discrepancy or distortion between two signals and is often utilized to assess the extent of quality degradation or distortion in domains such as image processing, video coding, and signal compression. Mahalanobis Distance measures the distances between points and distributions, and, by accounting for the covariance structure of the data, it provides a more accurate calculation of the distances between samples [13,14]. Compared to traditional distance metrics such as Euclidean Distance, DTW offers a more accurate measure of similarity between time series signals and is suitable for comparing the shape similarity between two time series [15]. It is widely utilized in fields such as speech recognition and handwriting recognition [16]. Tyler Dare applied the DTW algorithm in recognizing signals originating from various acoustic sources [17]. Guo improved the DTW algorithm for detecting bearing faults, achieving high levels of accuracy [18]. Liu proposed a Soft-DTW algorithm for

waveform inversion that can effectively avoid falling into local minima during the solution process [19]. Zhao proposed a shape Dynamic Time Warping (shapeDTW), which enhances DTW by taking point-wise local structural information into consideration [20].

In this research, the sine-fitting method was initially utilized to derive the reference signal [21]. Following this, a Normalized Dynamic Time-Warping (NDTW) algorithm is introduced for evaluating the stability of the acoustic field, entailing a comparison between the measured and reference signals. This transformation transforms the evaluation of acoustic field stability into a similarity issue between the measured and reference signals. The NDTW algorithm introduced in this research integrates length and amplitude calculations, thereby enabling it to identify discrepancies between measurement and reference signals with greater efficacy. The NDTW algorithm addresses the limitations of methods such as Cross Correlation and the Pearson Correlation Coefficient in effectively detecting minute differences in single-frequency signals with similar amplitudes. Furthermore, it resolves the computational errors caused by signal-length accumulation in methods like Euclidean Distance and Dynamic Time Warping, providing a unified and objective metric for measuring signals of varying lengths, amplitudes, and frequencies. An experiment in an anechoic water tank testing the calibration of hydrophones by an optical method was conducted. The calibration result for the signal within the frequency band identified by the NDTW algorithm as having good quality exhibits a deviation of no more than 0.7 dB from the reciprocity method.

The Section 2 of the manuscript introduces the principles of the NDTW method, including the use of sine fitting to obtain reference signals and a detailed explanation of the NDTW algorithm. The Section 3 describes the simulation and underwater experiments, which comprise an underwater acoustic-pressure signal-recognition experiment, recognition of signals with varying lengths, and hydrophone calibration using the optical method. Within the experiments, comparisons between the NDTW method and other approaches demonstrate that the NDTW method exhibits superior recognition capabilities which are unaffected by signal length or amplitude. Under conditions in which the NDTW identifies a stable acoustic field, the calibration results obtained using the optical method closely align with those derived from the reciprocity method. Finally, the Section 4 provides a comprehensive summary of the findings presented in this study.

2. Normalized DTW Algorithm

In assessing the stability of velocity within an acoustic field, a reliable reference signal is essential. Considering the varying frequencies and amplitudes inherent in the signals, this paper adopts a sine-fitting methodology to model the steady-state component of the measured signal. Consequently, a standardized sine wave signal is obtained, which is utilized as the reference signal. The assumed model for the measured signal is outlined as follows:

$$y(t) = A\sin(2\pi ft + \varphi) + C \tag{1}$$

where A denotes the amplitude of the measured signal and φ denotes the phase of the measured signal. Equation (1) can be rewritten as

$$y(t) = a\sin(2\pi ft) + b\cos(2\pi ft) + C \tag{2}$$

The amplitude and phase are calculated by

$$A = \sqrt{a^2 + b^2},\ \varphi = \arctan\left(\frac{b}{a}\right) \tag{3}$$

Assume the steady-state signal is represented as $(t_l, y_l), l = 1, \ldots, N$; the following approach is employed to perform sine-fitting on the steady-state signal, with the primary objective of minimizing errors. This mathematical operation can be formalized as follows:

$$\min S^2 = \sum_{l=1}^{N} (y_l - y(t_l))^2 \tag{4}$$

The reference signal, computed using the aforementioned sine-fitting method, is a sine wave with a stable amplitude that matches the frequency of the measured signal. When the numerical values of the reference signal and the measured signal are closely aligned at each point, the measured signal can be approximated as a stable sinusoidal signal. In such cases, the amplitude of the measured signal can be approximated by the amplitude of the reference signal. Conversely, if there is a substantial difference between the reference signal and the measured signal, it suggests that the velocity of the acoustic field is unstable and cannot be approximated as a stable sinusoidal signal.

To quantify the disparity between the reference signal and the measured signal, a localized distance metric is employed:

$$d : Y_l \times Y(t_l) \to R \geq 0 \tag{5}$$

Intuitively, the distance metric d assumes a small value when the signals Y_l and $Y(t_l)$ are similar and a large value when they are dissimilar. Consequently, the objective of assessing the similarity between the signals transforms into the challenge of arranging all sequence points in a manner that minimizes a cost function.

The algorithm is initiated by the construction of a distance matrix, $C \in R^{N \times M}$, which encapsulates all pairwise distances between the elements of sequences Y_l and $Y(t_l)$. This distance matrix is termed the local cost matrix and serves as the foundation for aligning Y_l and $Y(t_l)$:

$$C \in R^{N \times M} : c_{i,j} = \left\| y_i - y(t_j) \right\|, i \in [1:N], j \in [1:M] \tag{6}$$

The cost function associated with a warping path computed with respect to the local cost matrix is

$$c_p(Y_l, Y(t_l)) = \sum c(y_n, y(t_m)) \tag{7}$$

Given the non-uniqueness of the value of c_p, dynamic programming is utilized to determine the optimal solution. When the cost function reaches its minimum value, it represents the shortest path between points Y_l and $Y(t_l)$. The relevant formula is expressed as follows:

$$c_{p*}(Y_l, Y(t_l)) = \min\left\{ c_p(Y_l, Y(t_l)), p \in P^{N \times M} \right\} \tag{8}$$

When employing the dynamic programming method, it is unnecessary to compute all potential values of the cost function. Instead, one must select the minimum value within the local cost matrix along a specific direction to ascertain the minimal cost function value. This notion is depicted in the diagram presented as Figure 1.

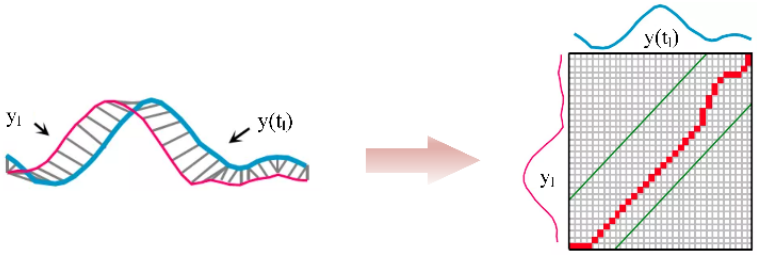


Figure 1. Schematic diagram of dynamic programming [22].

In Figure 1, the matrix beneath the curves Y_l and $Y(t_l)$ represents the local cost matrix. The red path illustrates the minimal cost function value, which corresponds to the optimal alignment path from the starting points of Y_l and $Y(t_l)$ to their endpoints, following a unidirectional trajectory.

Given the variations in amplitudes and lengths among the various velocity signals, a unified evaluation criterion is established, while ensuring that the differences between the measured signals and the reference signals are maintained. This criterion is achieved through normalization of both the reference signal and the measured signal, utilizing the amplitude A and length M of the reference signal as benchmarks. The normalization process mitigates the impact of signal amplitudes and lengths on the results, while preserving the relative characteristics of the measured signal y_l compared to the reference signal $y(t_l)$.

In summary, the normalized signal quality evaluation method proposed in this paper and named Normalized Dynamic Time Warping (NDTW), which is based on signal amplitude and signal length, is computed as detailed below.

$$\mathrm{NDTW} = \lg\left(\frac{1000}{M}\frac{\sqrt{\sum_{i=1}^{N}\min\left(y_i - y\left(t_j\right)\right)^2}}{A}\right), \mathrm{j} \in [i, M) \tag{9}$$

In Equation (9), lg is logarithm based on 10, $\sqrt{\sum_{i=1}^{N}\min\left(y_i - y\left(t_j\right)\right)^2}$ denotes the minimum distance between the signal y and $y(t)$. A represents the amplitude of the signal, which corresponds to the velocity of the pellicle, measured in units of m/s. M stands for the length of the signal, which is the total number of discrete points in the signal. The coefficient of 1000 is used to convert the units of the amplitude from the meter level (as used in the formula) to the millimeter level (as observed in actual measurements), since the velocity amplitude in practical scenarios is typically expressed at the millimeter level.

The NDTW algorithm calculates the minimum distance between signals using a dynamic approach. It begins by computing and unidirectionally accumulating the local minimum distances; this is followed by normalizing the amplitude and length of the signals. This normalization eliminates the influences of amplitude and length on distance calculations. The NDTW algorithm functions as an indicator of the relative similarity between a measured signal and a reference signal. It offers a standardized evaluation metric that is adaptable for signals with varying frequencies, lengths, and amplitudes, allowing for consistent comparisons across diverse datasets. A lower NDTW value indicates a higher level of similarity between the two signals.

3. Simulations and Experiments

To validate the proposed algorithm, we conducted simulations and experiments, comparing the performance of the Normalized Dynamic Time-Warping (NDTW) method against various performance evaluation metrics, including the Dynamic Time Warping (DTW), Peak Signal-to-Noise Ratio (PSNR), Mean Squared Error (MSE), Euclidean Distance (ED), Xcorr, Pearson Correlation Coefficient, Jaccard–Tanimoto Coefficient, and Mahalanobis Distance methods.

3.1. Numerical Simulations

The correspondence between NDTW and signal stability has been established through numerical simulations. The simulated setup comprises a laser carrier with a frequency of 40 MHz and a wavelength of 632.7 nanometers. The simulated velocity signals encompass

frequencies of 50 kHz, 100 kHz, and 150 kHz, each with a velocity amplitude of 0.1 mm. Gaussian white noise was introduced into the simulations to achieve a signal-to-noise ratio of 40 dB. The demodulated results of these simulated signals are presented in Figure 2, while the evaluation metrics for the measured signals are summarized in Figure 3.

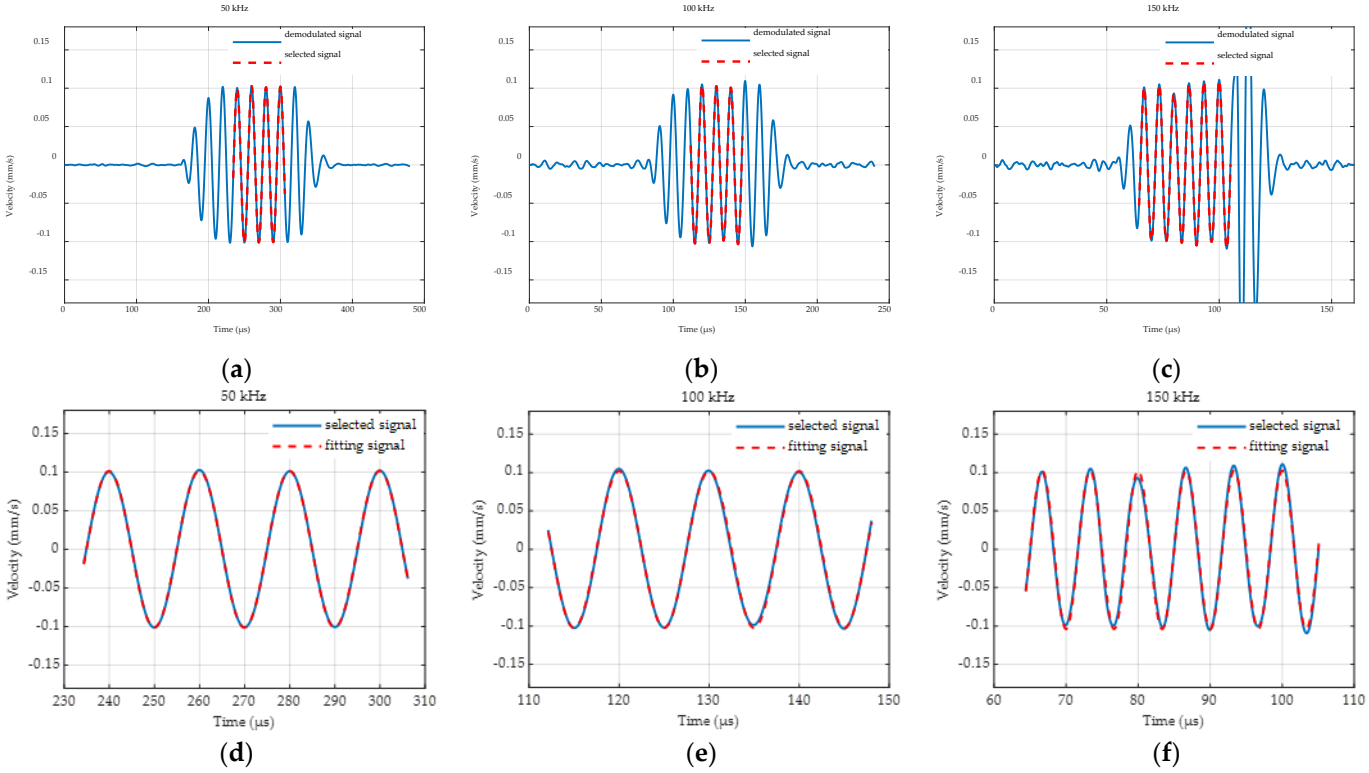


Figure 2. Simulation signal, experimental results: (**a**) 50 kHz demodulated signal and selected signal; (**b**) 100 kHz demodulated signal and selected signal; (**c**) 150 kHz demodulated signal and selected signal; (**d**) 50 kHz selected signal and fitting signal; (**e**) 100 kHz selected signal and fitting signal; and (**f**) 150 kHz selected signal and fitting signal.

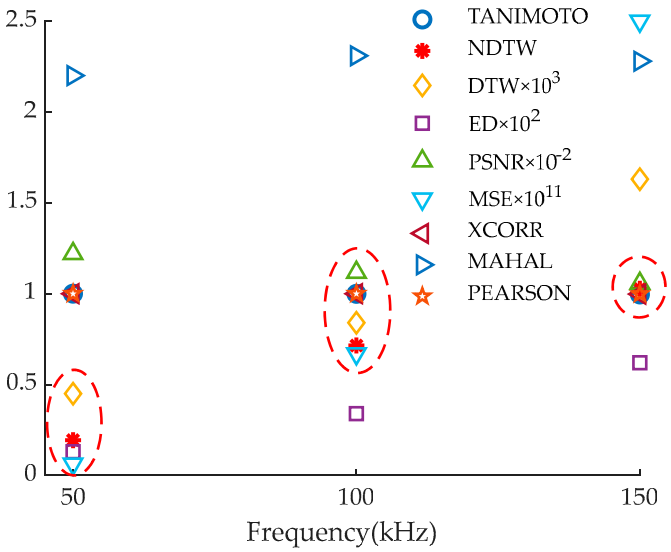


Figure 3. Results of simulated signals using different algorithms.

To enhance the intuitive presentation of data, the outcomes of certain calculation methodologies, including DTW, ED, PSNR, and MSE, have been scaled.

Figure 3 presents the results calculated by the NDTW, DTW, ED, PSNR, MSE, Xcorr, Pearson Correlation Coefficient, Jaccard–Tanimoto Coefficient, and Mahalanobis Distance methods for simulated signals at 50 kHz, 100 kHz, and 150 kHz frequencies. As the frequency of the simulated signals increases, the magnitude of signal fluctuation progressively augments, with the 150 kHz signal exhibiting the most pronounced and unstable fluctuations.

Among them, the calculation results of the Xcorr, Pearson Correlation Coefficient, Jaccard–Tanimoto Coefficient, and Mahalanobis Distance methods fail to make significant distinctions between various signals. This is attributed to the high similarity associated with the reference signal, which is fitted from the measured signal, rendering it challenging to make effective distinctions directly through similarity calculation methods. Given the high similarity between the reference signal and the measured signal, their PSNR is correspondingly high, rendering the PSNR method ineffective for accurate recognition. The NDTW, DTW, ED, and MSE methods measure the distance between the reference signal and the measured signal, enabling them to accurately discern small differences between the two. Furthermore, the NDTW method exhibits a consistent trend with DTW, ED, and MSE in recognizing various signals. The simulation results demonstrate that the NDTW method proposed in this study effectively identifies small differences between measured signals and reference signals, with the identification results aligning with those of other comparative methods.

Based on the results obtained from these simulations, the following evaluation criteria for the NDTW method are established: an NDTW value less than 1 indicates that the measured signals are stable, whereas an NDTW value greater than 1 indicates instability in the measured signals.

3.2. Underwater Experiments

To further validate the recognition method of the NDTW algorithm, a series of underwater experiments were conducted. Initially, underwater velocity measurement experiments were designed to ascertain the effective recognition capability of NDTW for velocity signals. Subsequently, experiments for the calibration of hydrophones by an optical method were developed to investigate the correlation between the outcomes of NDTW and the sensitivity of the hydrophones. The underwater acoustic pressure measured by the optical method was conducted within an anechoic water tank, as depicted in Figure 4.

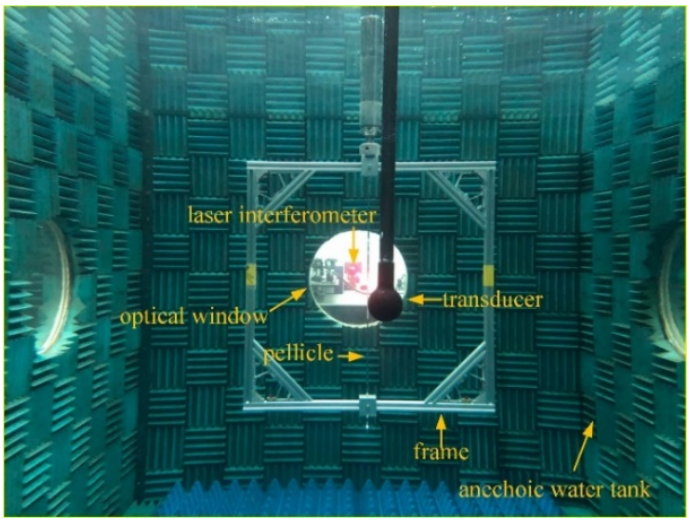


Figure 4. Underwater acoustic-pressure measurement system.

Figure 5 presents a schematic diagram illustrating the measurement of underwater acoustic pressure using a laser heterodyne interferometer. A signal generator produces a driving signal that is subsequently amplified by a power amplifier. The amplified signal drives the transducer to generate vibrations, which in turn induce vibrations in the medium and the pellicle. These vibrations in the pellicle create a Doppler effect in the laser beam, converting the optical signal into a voltage signal. The Zero-Crossing algorithm is then employed to demodulate this voltage signal and calculate the velocity. By combining the velocity data $u(t)$ with the underwater acoustic velocity c and density ρ, the underwater acoustic pressure can be calculated with the function $P(t) = \rho c u(t)$. This approach constitutes the optical method for measuring underwater acoustic pressure.

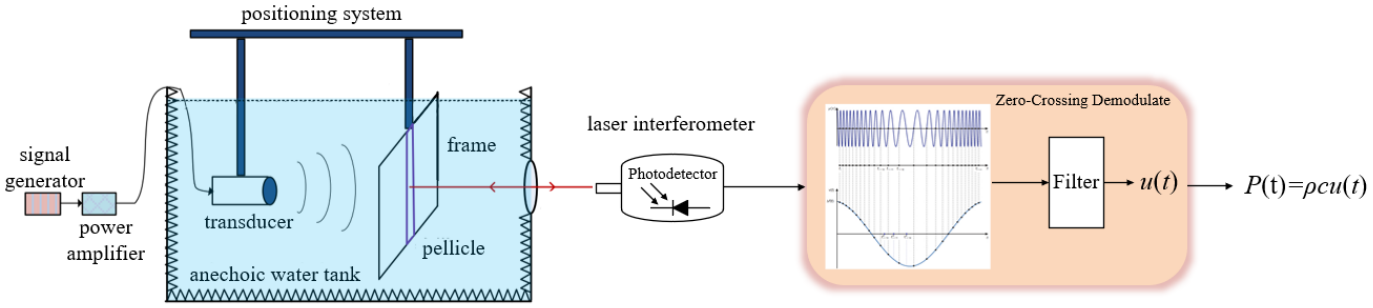


Figure 5. Schematic diagram of underwater acoustic pressure measured by the optical method.

3.2.1. Underwater Acoustic-Pressure Signal-Recognition Experiment

In the evaluation of underwater acoustic-pressure signal quality, it is only necessary to measure the velocity signal of the pellicle. The velocity signal is subjected to sine fitting to generate a reference signal, which is then employed in the NDTW algorithm to assess signal quality.

In the experiment, the transducer's output frequency ranged from 30 kHz to 180 kHz, with intervals of 10 kHz. Notably, the operating frequency of the transducer did not exceed 130 kHz. To enhance the comparability of the algorithm, this study retained the unstable signals. By demodulating the laser signal, the velocity signal was obtained; this value reflects the underwater acoustic pressure.

The velocity signal of the pellicle can be categorized into three components: the transient signal, the steady-state signal, and the tail signal. The transient signal arises from the transducer's transient response, while the steady-state signal represents the sinusoidal velocity driven by the transducer. The tail signal, on the other hand, reflects the velocity of the pellicle due to its elasticity after the transducer ceases operation. After selecting the stable segment of the signal, a sine-fitting technique is employed to compute the reference signal [10]. An excerpt of the velocity signal is depicted in Figure 6.

The measured results reveal that the initial one to two waves exhibit amplitude instability, which can be traced back to transient signals stemming from the transducer's transient response. Following this, there emerges a segment of steady-state signal with a stable amplitude, succeeded by a tail signal with a significantly diminished amplitude. To accurately characterize the velocity state of the pellicle, it is imperative to select the steady-state signal segment and fit it to compute the reference signal. The resultant data are presented in Figure 7.

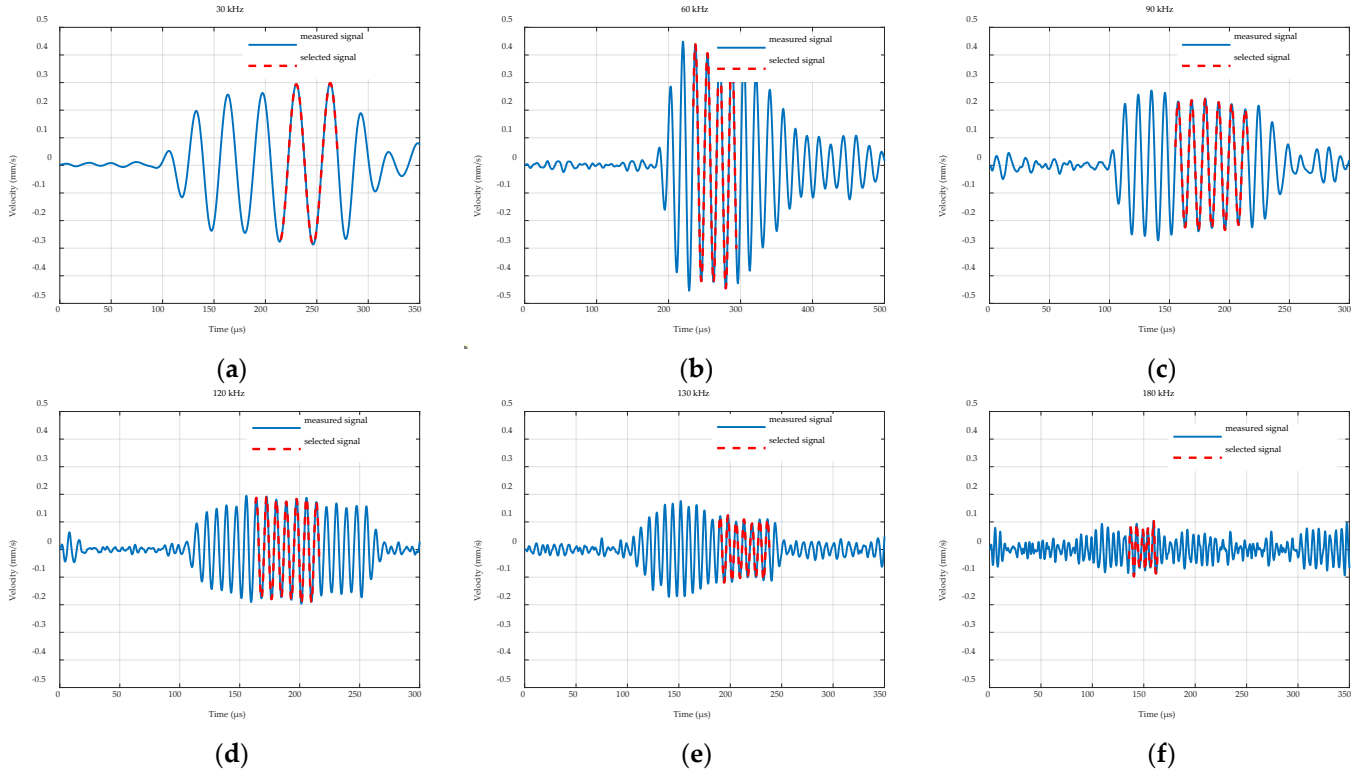


Figure 6. Different frequencies of velocity signals: (**a**) 30 kHz measured signal and selected signal; (**b**) 60 kHz measured signal and selected signal; (**c**) 90 kHz measured signal and selected signal; (**d**) 120 kHz measured signal and selected signal; (**e**) 130 kHz measured signal and selected signal; and (**f**) 180 kHz measured signal and selected signal.

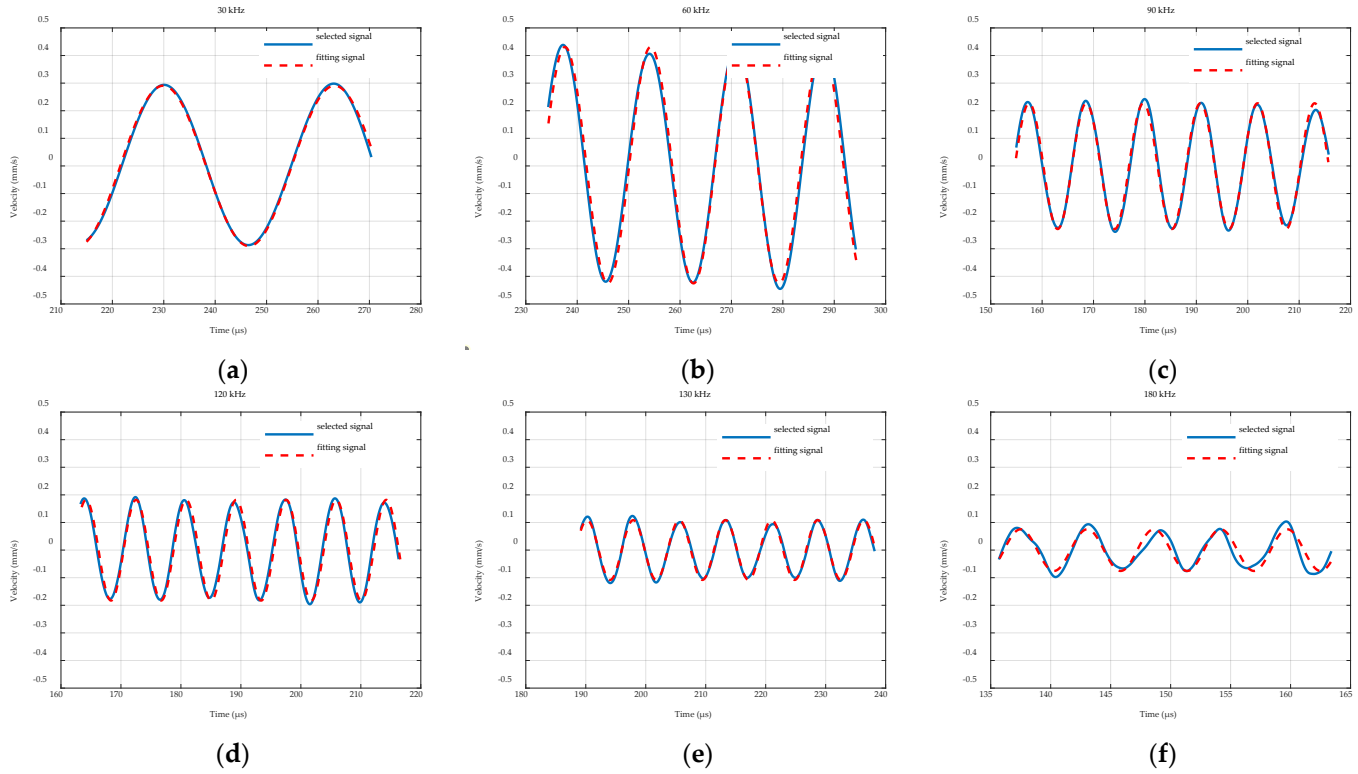


Figure 7. Different frequencies of fitting signals: (**a**) 30 kHz selected signal and fitting signal; (**b**) 60 kHz selected signal and fitting signal; (**c**) 90 kHz selected signal and fitting signal; (**d**) 120 kHz selected signal and fitting signal; (**e**) 130 kHz selected signal and fitting signal; and (**f**) 180 kHz selected signal and fitting signal.

Due to the operational frequency constraints of the transducer, which range from 130 kHz to 180 kHz, it is impossible to maintain a stable acoustic field. Consequently, the velocity signals exhibit significant fluctuations. In the experiments conducted in this paper, the NDTW algorithm demonstrated its efficacy in identifying unstable signals. A comparison of the results obtained with other conventional evaluation algorithms is presented in Figure 8. Table 1 shows the results of the data in Figure 8 without magnification.

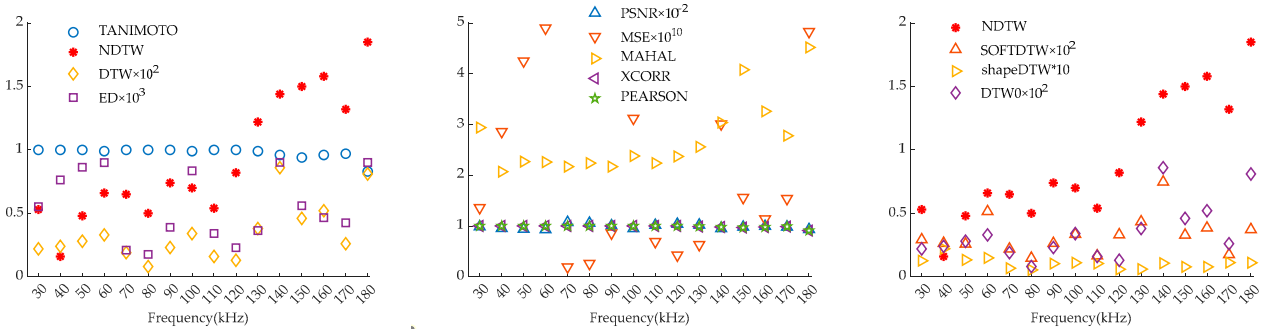


Figure 8. Evaluation metric values within the frequency range of 30 to 180 kHz: (**a**) values for the Jaccard–Tanimoto Coefficient, NDTW, DTW, and ED; (**b**) values for the PSNR, MSE, Mahalanobis Distance, Cross Correlation and Pearson Correlation Coefficient; (**c**) values for the NDTW, DTW, Soft-DTW, and shape-DTW.

Table 1. Evaluation metric values within the frequency range of 30 to 180 kHz.

Frequency (kHz)	DTW	ED	NDTW	PSNR	MSE	xcorr	Mahal	Pearson	SOFT-DTW	ShapeDTW
30	0.0022	5.52×10^{-4}	0.53	98.68	1.36×10^{-10}	1.00	2.94	1.00	0.0029	0.0126
40	0.0024	7.63×10^{-4}	0.16	95.44	2.86×10^{-10}	1.00	2.07	1.00	0.0026	0.0220
50	0.0028	8.63×10^{-4}	0.48	93.72	4.25×10^{-10}	1.00	2.27	1.00	0.0026	0.0133
60	0.0033	9.00×10^{-4}	0.66	93.09	4.90×10^{-10}	1.00	2.26	1.00	0.0051	0.0149
70	0.0019	2.10×10^{-4}	0.65	107.17	1.92×10^{-11}	1.00	2.17	1.00	0.0022	0.0067
80	0.0008	1.76×10^{-4}	0.50	105.87	2.59×10^{-11}	1.00	2.24	1.00	0.0015	0.0054
90	0.0023	3.90×10^{-4}	0.74	100.66	8.59×10^{-11}	1.00	2.17	1.00	0.0026	0.0104
100	0.0034	8.35×10^{-4}	0.70	95.05	3.12×10^{-10}	1.00	2.38	1.00	0.0033	0.0110
110	0.0016	3.41×10^{-4}	0.54	101.61	6.91×10^{-11}	1.00	2.24	1.00	0.0017	0.0104
120	0.0013	2.29×10^{-4}	0.82	103.73	4.24×10^{-11}	1.00	2.37	1.00	0.0033	0.0059
130	0.0038	3.64×10^{-4}	1.22	102.00	6.31×10^{-11}	0.99	2.56	0.99	0.0043	0.0060
140	0.0086	9.02×10^{-4}	1.44	95.21	3.01×10^{-10}	0.98	3.04	0.98	0.0075	0.0107
150	0.0046	5.60×10^{-4}	1.50	98.07	1.56×10^{-10}	0.97	4.08	0.97	0.0033	0.0078
160	0.0052	4.66×10^{-4}	1.58	99.42	1.14×10^{-10}	0.98	3.26	0.98	0.0038	0.0078
170	0.0026	4.25×10^{-4}	1.32	98.12	1.54×10^{-10}	0.99	2.78	0.99	0.0018	0.0112
180	0.0081	9.01×10^{-4}	1.85	93.16	4.83×10^{-10}	0.91	4.52	0.91	0.0037	0.0111

As illustrated in Figure 8, the Jaccard–Tanimoto Coefficient, Pearson Correlation Coefficient, Cross Correlation, and PSNR methods produce nearly identical results across various frequencies, rendering it challenging to discern differences between the measured signals and the reference signals. This is primarily attributable to the structural similarity between the reference signal and the measured signal, rendering the aforementioned methods ineffective in detecting minor differences. Nevertheless, the results of the DTW, ED and MSE methods are discrete, which obstructs the effective distinction between various signals and, consequently, prevents an accurate assessment of acoustic field stability. The Mahalanobis Distance demonstrates stable identification results for frequencies ranging from 40 kHz to 120 kHz. However, for the 30 kHz signal, the identification results are remarkably similar to those of 140 kHz and 170 kHz signals. This similarity arises because, for shorter signal lengths, the Mahalanobis Distance tends to produce inaccurate identification results. The shapeDTW algorithm did not exhibit significant differentiation, while the softDTW demonstrated trends similar to those of DTW. This similarity arises from the

fact that softDTW merely optimizes the alignment path without fundamentally altering the underlying distance computation. This is primarily because these methods neglected the impact of signal length on the calculation results. The NDTW method accounts for this factor and mitigates the influence of signal-length accumulation. Consequently, the final calculation reveals a significant difference in the velocity of the measured signal on either side of NDTW = 1, indicating variations in acoustic field stability.

Based on the findings of the NDTW analysis, for frequencies below 130 kHz where NDTW values are less than 1, the amplitude of the measured signal remains consistent across different cycles, indicating stable velocity within the acoustic field. For frequencies above 130 kHz where NDTW values exceed 1, a notable difference in the amplitude of the measured signal is observed across different cycles, signifying unstable velocity within the acoustic field. Consequently, the NDTW method serves as an accurate tool for identifying amplitude differences in measured signals across different periods and assessing the stability of the acoustic field, which is essential for calibration purposes.

3.2.2. The Results of Signals with Different Length

The experimental of acoustic pressure measured by optical method indicate that the NDTW method exhibits superior efficacy in distinguishing measured signals compared to alternative methodologies.

To further validate the recognition capability of NDTW in relation to signals of varying lengths, we selected three distinct signal durations from steady-state signal segments with the frequencies of 100 kHz and 180 kHz, namely, short, medium, and long signal segments. Subsequently, we applied algorithms to assess their velocity stability.

For each frequency, three waveforms of different lengths are selected for calculation, as shown in Figure 9. The calculation results of each method are shown in Figure 10.

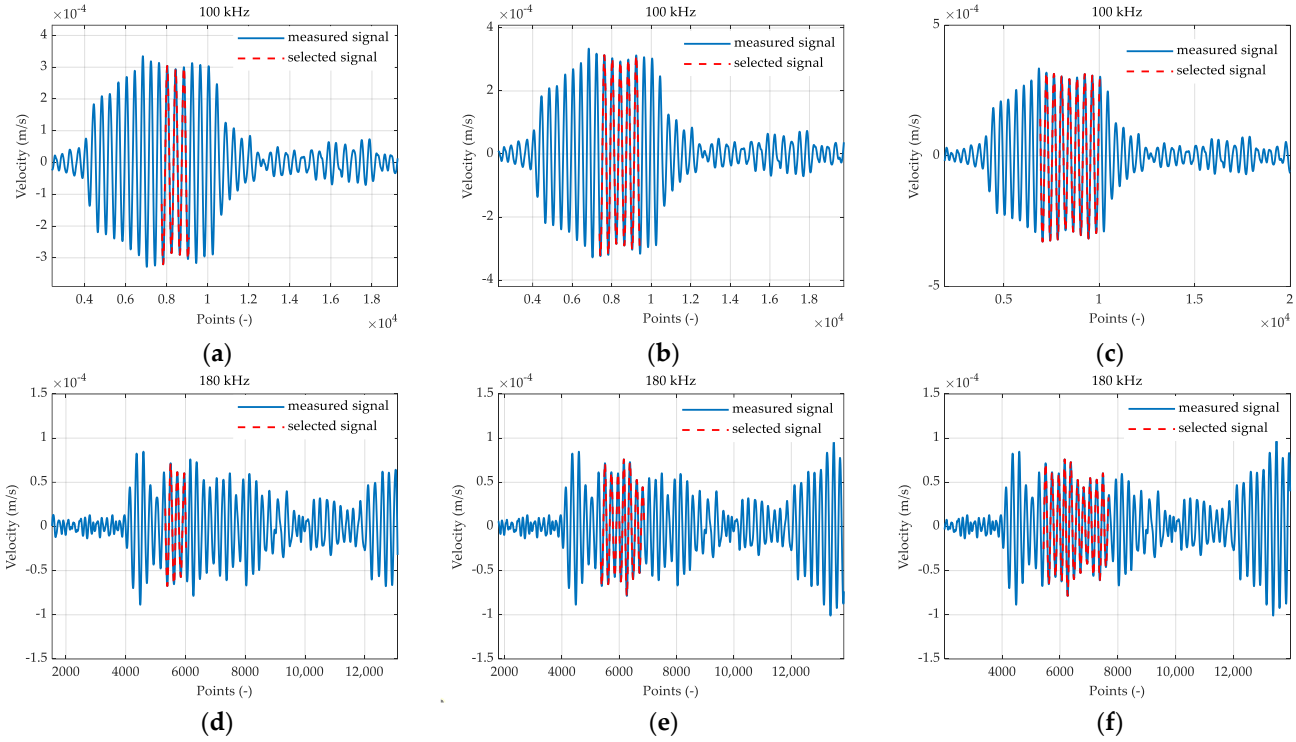


Figure 9. Selection of different signal lengths for 100 kHz and 180 kHz: (**a**) 100 kHz with short signal sequence; (**b**) 100 kHz with medium signal sequence; (**c**) 100 kHz with long signal sequence; (**d**) 180 kHz with short signal sequence; (**e**) 180 kHz with medium signal sequence; and (**f**) 180 kHz with long signal sequence.

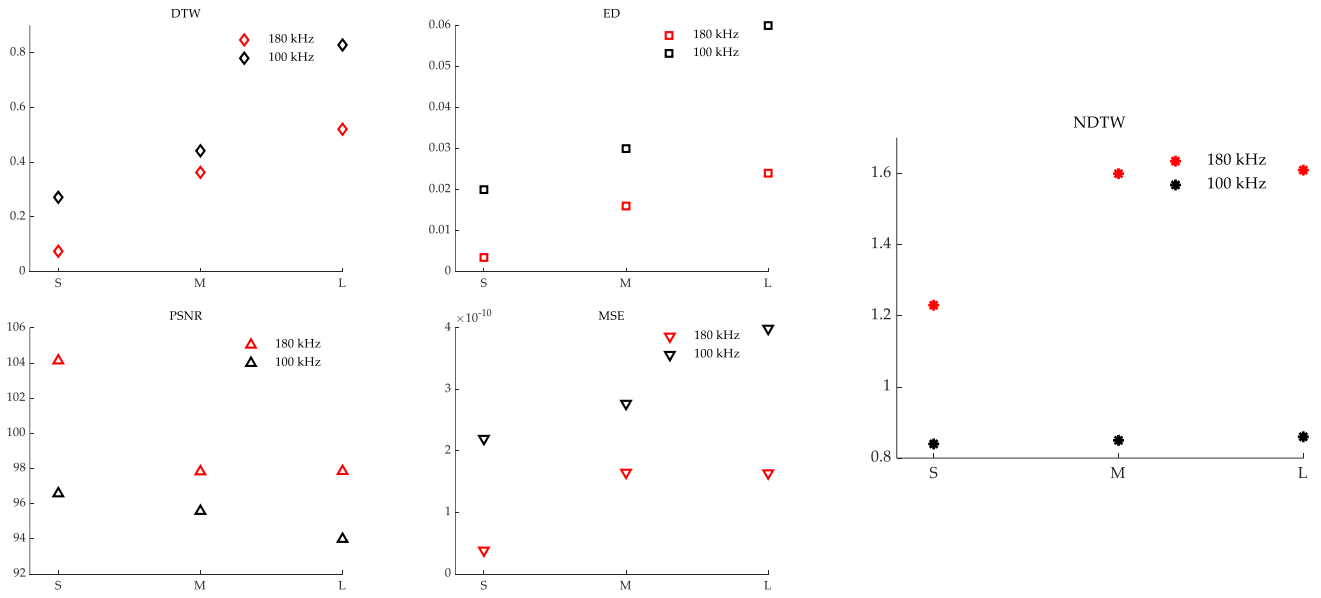


Figure 10. Calculation results for signals of different lengths, using different methods: (**a**) values of DTW, ED, PSNR, and MSE; (**b**) values of NDTW.

In Figures 9 and 10, the velocity of the acoustic field at 100 kHz exhibits relative stability. By selecting steady-state signals of varying lengths for computation, the results obtained using the NDTW method remain consistent. Conversely, the stability of the acoustic field velocity at 180 kHz is poor, and discrepancies arise in the NDTW results when different signal lengths are selected. Despite this, accurate identification of the signal is still feasible. Specifically, as shown in Figure 9d, a signal with three cycles was chosen. Owing to the signal's short length, the difference between the reference signal and the measured signal is minimal, yet the stability of the measured signal can still be discerned effectively. As the selected signal length increases, the recognition results obtained through NDTW become increasingly consistent.

3.2.3. The Experiments Relating to the Calibration of Hydrophones

In the calibration of hydrophones utilizing optical methods, the underwater acoustic pressure is determined by the velocity of the pellicle. Following this, the output voltage of the hydrophone is measured at the location identical to that where the pellicle is positioned. The sensitivity of the hydrophone is calculated as the ratio of its output voltage to the underwater acoustic pressure. The method proposed in this study focuses on evaluating the quality of velocity within the acoustic field. Given that the pellicle is capable of tracking the vibrations of water particles, the signal it emits can serve as an indicator of the vibrations occurring within the acoustic field. Currently, there is no direct quantitative relationship between NDTW and the sensitivity of hydrophones. This study presents a comparative experiment that analyzes the calibration of hydrophones, using the optical method versus the reciprocity method. The findings of the comparative experiment are illustrated in Figure 11.

Figure 11 presents the calibration results for hydrophone sensitivity and the identification results obtained using the NDTW method. The red curve represents the results from the optical method, with an error margin of 0.5 dB, while the black curve shows the results from the reciprocity method, with an error margin of 0.7 dB. In the calibration of the hydrophone by the optical method, the NDTW method was employed to compute the sound pressure signal, with the computed results represented by circular scatter points in

the figure. Black circles indicate NDTW results less than 1, while red circles denote NDTW results greater than 1.

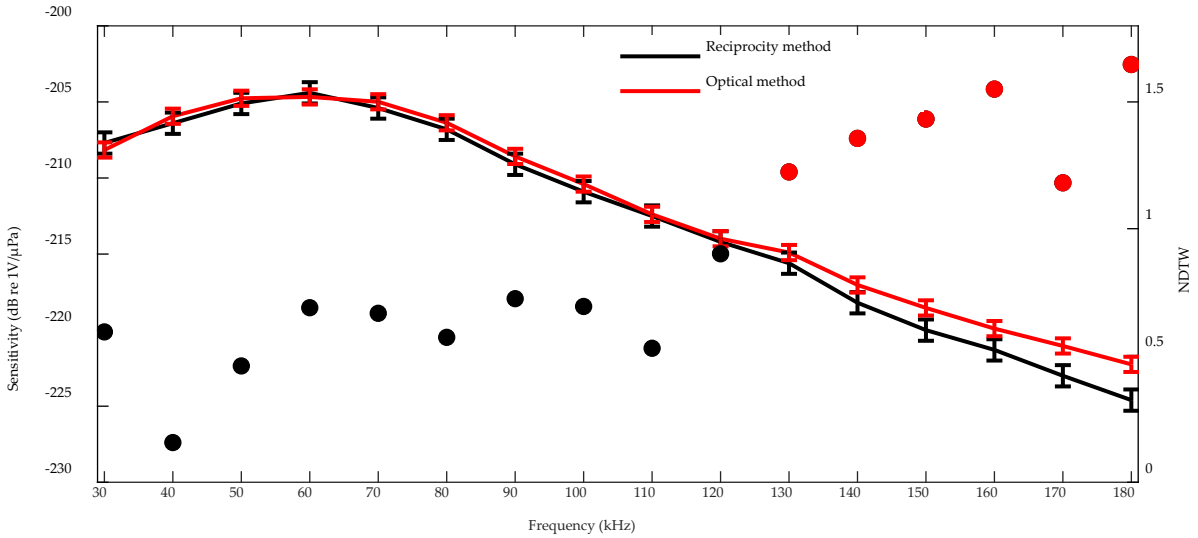
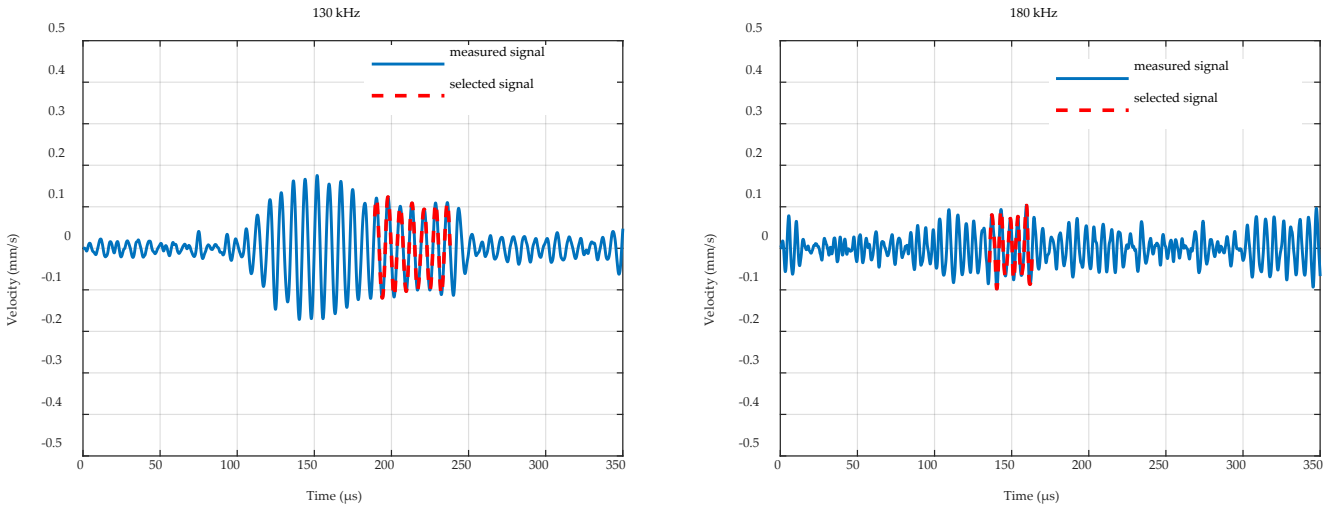


Figure 11. The result of calibrations with the optical method and the reciprocity method.

As illustrated in Figure 11, it is apparent that when the NDTW is less than 1, the sensitivity differences between the calibrations performed using the optical method and those performed using the reciprocity method do not exceed 0.7 dB. Conversely, when the NDTW surpasses 1, the sensitivity discrepancies between the two methods exceed 0.7 dB, surpassing the uncertainty associated with the reciprocity method. Additionally, within these frequency bands, the vibration velocity signals demonstrate notable instability, as exemplified by the signals at 130 kHz and 180 kHz shown in Figure 12.



(**a**) (**b**)

Figure 12. The waveform of pellicle velocity at 130 kHz and 180 kHz: (**a**) 130 kHz velocity signal; (**b**) 180 kHz velocity signal.

From Figure 12, it is evident that the velocity signals at frequencies of 130 kHz and 180 kHz exhibit notable fluctuations, which make it difficult to meet the stable acoustic field for hydrophone calibration. Consequently, the hydrophone sensitivity calibrated under the resulting conditions is characterized by a high degree of uncertainty, thereby undermining the reliability of the calibration process. This demonstrates the effectiveness of the NDTW

algorithm in the optical calibration of hydrophones and its potential to be utilized as a reference for evaluating the reliability of the calibration results.

4. Discussion

The NDTW algorithm was utilized in the calibration of hydrophones by laser interferometry within a frequency range of 30-180 kHz. The results obtained were subsequently compared with those derived from the reciprocity method. The calibration result for the signal within the frequency band identified by the NDTW algorithm as having good quality exhibits a deviation of no more than 0.7 dB from the reciprocity method. Conversely, the frequency band identified by the NDTW algorithm exhibits a relatively poor signal quality, resulting in a calibration result that deviates substantially from the reciprocity method, with the deviation exceeding 0.7 dB. This demonstrates the effectiveness of the NDTW algorithm in the optical calibration of hydrophones and its potential to enhance the accuracy of the calibration results. The calibration of hydrophones with the optical method directly measures the pressure of the acoustic field, allowing the NDTW method to evaluate the acoustic field. By analyzing the NDTW calculation results, the stability of the sound field can be assessed, thereby enhancing the accuracy and the reliability of the calibration outcomes.

5. Conclusions

The NDTW algorithm introduced in this paper is tailored to assess the stability of the acoustic field in the calibration of hydrophones by optical technology. Utilizing a transparent pellicle to measure underwater acoustic pressure allows for the acquisition of data on acoustic-pressure variations. By employing the sine-fitting method to derive the reference signal and subsequently comparing it with the measured signal, a deeper insight into the stability of acoustic field can be gained. A close correspondence between the signals signifies stable sinusoidal vibration, whereas significant discrepancies indicate instability.

In comparison to commonly used signal quality assessment algorithms, the NDTW algorithm normalizes the amplitude and length of the signals, which can ensure the different signals have unified evaluation criterion. This unique feature mitigates recognition inaccuracies arising from variations in duration and amplitude. Consequently, the NDTW algorithm boasts a broader range of applicability and attains the highest level of recognition accuracy.

Currently, the value calculated by the NDTW method proposed in the paper does not have a direct relation with the result of calibration. Future work will focus on establishing a quantitative relationship between the NDTW calculation results and the stability of the sound field. Additionally, further exploration will be conducted to evaluate the impact of NDTW on hydrophone calibration outcomes.

Author Contributions: Conceptualization, X.L.; Data curation, H.Z.; Formal analysis, X.L.; Funding acquisition, P.Y.; Investigation, X.L. and M.W.; Methodology, X.L.; Resources, P.Y., K.W. and L.H.; Software, X.L.; Supervision, H.Z., P.Y., K.W. and L.H.; Validation, X.L.; Visualization, H.Z. and M.W.; Writing—original draft, X.L.; Writing—review and editing, H.Z. and M.W. All authors have read and agreed to the published version of the manuscript.

Funding: This research was funded by National Key R&D Program of China (2022YFF0607503); National Natural Science Foundation of China (NSFC) (51805506); and Fundamental Research Funds of National Institute of Metrology (AKYTC1601).

Data Availability Statement: Dataset available on request from the authors.

Conflicts of Interest: The authors declare no conflicts of interest.

References

1. Drain, L.E. The Laser Doppler Techniques. 1980. Available online: https://ui.adsabs.harvard.edu/abs/1980wi...book.....D (accessed on 31 December 2024).
2. Abbas, S.H.; Jang, J.-K.; Kim, D.-H.; Lee, J.-R. Underwater vibration analysis method for rotating propeller blades using laser Doppler vibrometer. *Opt. Lasers Eng.* **2020**, *132*, 106133. [CrossRef]
3. Jang, J.; Liu, P.; Kim, B.; Kim, S.; Sohn, H. Silicon wafer crack detection using nonlinear ultrasonic modulation induced by high repetition rate pulse laser. *Opt. Lasers Eng.* **2020**, *129*, 106074. [CrossRef]
4. Wang, Q.; Zhu, J.; Dai, J.; Fu, S.; Luo, X.; Feng, H. Research on blade modal testing method based on 3D scanning laser Doppler vibration measurement technology. In Proceedings of the 2nd International Conference on Electronic Science and Automation Control, Suzhou, China, 16–17 May 2020; pp. 16–17.
5. Peng, S.; Wu, S.; Li, Y.; Chen, H. All-fiber monostatic pulsed laser Doppler vibrometer: A digital signal processing method to eliminate cochannel interference. *Opt. Laser Technol.* **2020**, *124*, 105952. [CrossRef]
6. Wang, M.; Koukoulas, T.; Xing, G.; He, L.; Yue, Z. Measurement of underwater acoustic pressures in the frequency range 100 to 500 kHz using optical interferometry and discussion on associated uncertainties. In Proceedings of the 25th International Congress on Sound and Vibration, Hiroshima, Japan, 8–12 July 2018.
7. Koukoulas, T.; Theobald, P.; Robinson, S.P.; Hayman, G.; Moss, B. Particle velocity measurements using heterodyne interferometry and Doppler shift demodulation for absolute calibration of hydrophones. In Proceedings of the ECUA 2012 11th European Conference on Underwater Acoustics, Edinburgh, UK, 2–6 July 2012; p. 070022. [CrossRef]
8. Theobald, P.; Robinson, S.; Thompson, A. The Calibration of Hydrophones by a Novel Optical Technique in the Frequency Range 10 kHz TO 600 kHz. In Proceedings of the International Conference "Underwater Acoustic Measurements: Technologies & Results", Heraklion, Greece, 28 June–1 July 2005.
9. Theobald, P.D.; Robinson, S.P.; Thompson, A.D.; Preston, R.C.; Lepper, P.A.; Yuebing, W. Technique for the calibration of hydrophones in the frequency range 10 to 600 kHz using a heterodyne interferometer and an acoustically compliant membrane. *J. Acoust. Soc. Am.* **2005**, *118*, 3110–3116. [CrossRef]
10. Costa, L.D.F. Comparing cross correlation-based similarities. *arXiv* **2021**, arXiv:211108513.
11. Benesty, J.; Chen, J.; Huang, Y. On the importance of the Pearson correlation coefficient in noise reduction. *IEEE Trans. Audio Speech Lang. Process.* **2008**, *16*, 757–765. [CrossRef]
12. Chung, N.C.; Miasojedow, B.; Startek, M.; Gambin, A. Jaccard/Tanimoto similarity test and estimation methods for biological presence-absence data. *BMC Bioinform.* **2019**, *20* (Suppl. S15), 644. [CrossRef] [PubMed]
13. De Maesschalck, R.; Jouan-Rimbaud, D.; Massart, D.L. The mahalanobis distance. *Chemom. Intell. Lab. Syst.* **2000**, *50*, 1–18. [CrossRef]
14. Leys, C.; Klein, O.; Dominicy, Y.; Ley, C. Detecting multivariate outliers: Use a robust variant of the Mahalanobis distance. *J. Exp. Soc. Psychol.* **2018**, *74*, 150–156. [CrossRef]
15. Senin, P. *Dynamic Time Warping Algorithm Review*; University of Hawaii at Manoa: Honolulu, HI, USA, 2008.
16. Ratković, M.; Marijan, M.; Miljković, T.; Bjelić, M. Metoda za segmentaciju muzičkog signala na osnovu matrice samosličnosti. *Zb. Rad. Istočno Sarajevo* **2023**. Available online: https://www.etran.rs/2023/E_ZBORNIK_ETRAN_2023/ETRAN23_RADOVI/AK1.3.pdf. (accessed on 1 November 2024).
17. Dare, T. Dynamic time warping for transient noise classification. In *INTER-NOISE and NOISE-CON Congress and Conference Proceedings*; Institute of Noise Control Engineering: Wakefield, MA, USA, 2023; pp. 1116–1125.
18. Guo, J.; Si, Z.; Liu, Y.; Li, J.; Li, Y.; Xiang, J. Dynamic time warping using graph similarity guided symplectic geometry mode decomposition to detect bearing faults. *Reliab. Eng. Syst. Saf.* **2022**, *224*, 108533. [CrossRef]
19. Liu, Y.; Tang, J.; Tang, Z.; Sun, C. Robust full-waveform inversion based on automatic differentiation and differentiable dynamic time warping. *J. Geophys. Eng.* **2023**, *20*, 549–564. [CrossRef]
20. Zhao, J.; Itti, L. shapeDTW: Shape Dynamic Time Warping. *Pattern Recognit.* **2018**, *74*, 171–184. [CrossRef]
21. Robinson, S.P.; Hayman, G.; Harris, P.M.; Beamiss, G.A. Signal-modelling methods applied to the free-field calibration of hydrophones and projectors in laboratory test tanks. *Meas. Sci. Technol.* **2018**, *29*, 085001. [CrossRef]
22. Rakthanmanon, T.; Campana, B.; Mueen, A.; Batista, G.; Westover, B.; Zhu, Q.; Zakaria, J.; Keogh, E. Searching and mining trillions of time series subsequences under dynamic time warping. In Proceedings of the 18th ACM SIGKDD International Conference on Knowledge Discovery and Data Mining, Beijing, China, 12–16 August 2012; pp. 262–270. [CrossRef]

Disclaimer/Publisher's Note: The statements, opinions and data contained in all publications are solely those of the individual author(s) and contributor(s) and not of MDPI and/or the editor(s). MDPI and/or the editor(s) disclaim responsibility for any injury to people or property resulting from any ideas, methods, instructions or products referred to in the content.